Molecular Cell, Volume *32*

Supplemental Data

Structure and Substrate Recruitment of the Human Spindle Checkpoint Kinase Bub1

Jungseog Kang, Maojun Yang, Bing Li, Wei Qi, Chao Zhang, Kevan M. Shokat, Diana R. Tomchick, Mischa Machius, and Hongtao Yu

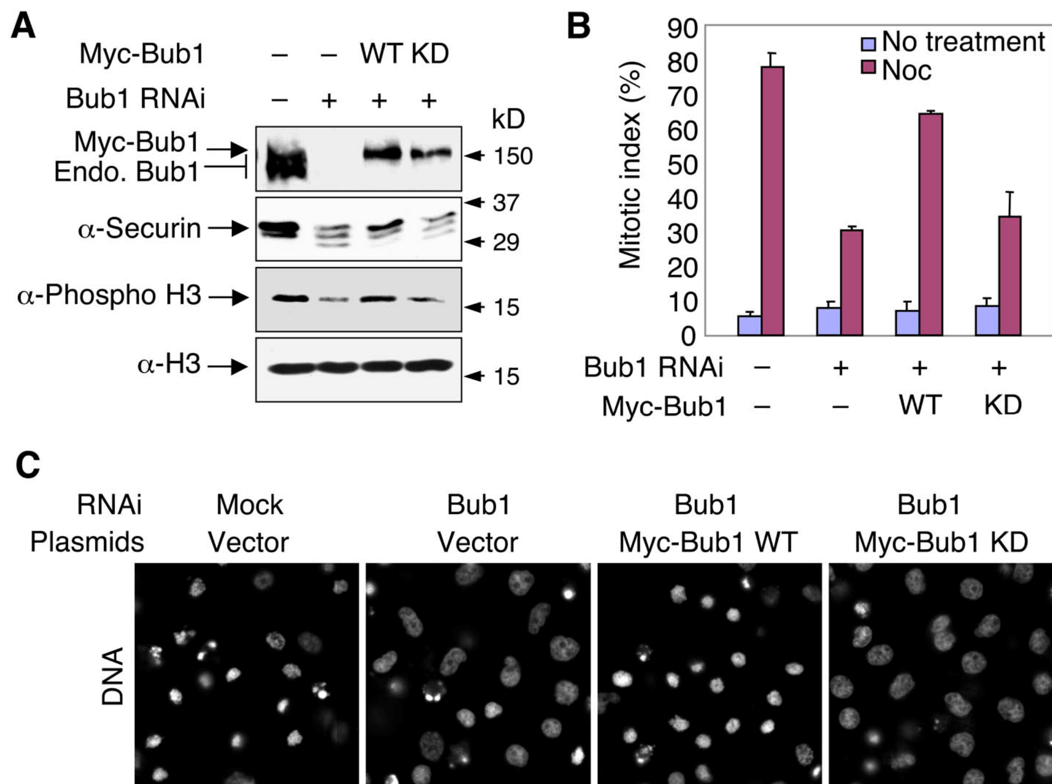

Figure S1. The Bub1 Kinase Activity Is Required for the Spindle Checkpoint

(A) HeLa tet-on cells were transfected with Bub1 siRNA along with RNAi-resistant Myc-Bub1 wild-type (WT) or kinase-dead (KD) vectors and then treated with nocodazole. The cell lysates were blotted with the indicated antibodies. The positions of Myc-Bub1 and the endogenous (Endo.) Bub1 are indicated.
(B) The mitotic indices of the cells described in (A). About 300 cells from three independent experiments were counted. The averages and standard deviations are shown.
(C) Cells described in (A) were incubated with Hoechst 33342 for 30 min and directly visualized using an inverted fluorescence microscope. The DNA morphology is shown.

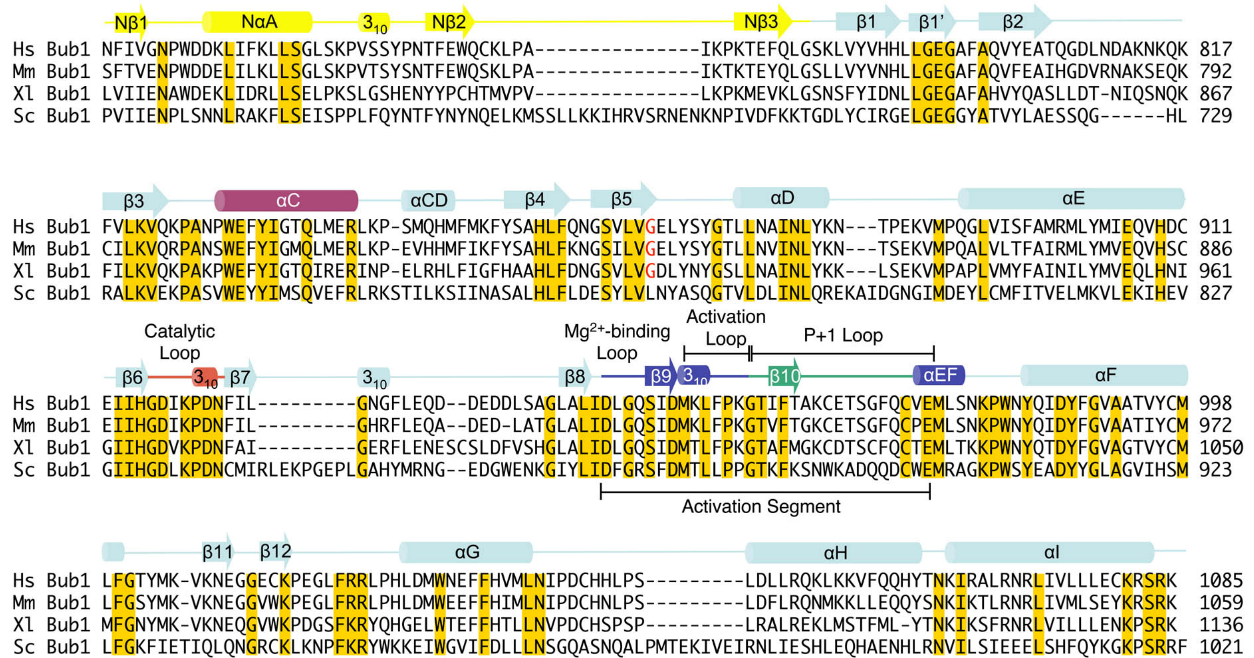

Figure S2. Sequence Alignment of the Extended Kinase Domain of Bub1

Identical residues are shaded yellow. Hs, *Homo sapiens*; Mm, *Mus musculus*; Xl, *Xenopus laevis*; Sc, *Saccharomyces cerevisiae*. The secondary structure elements are indicated on top. The positions of the catalytic loop, the Mg^{2+}-binding loop, the activation loop, and the P+1 loop are indicated. G866 in human Bub1 is colored red.

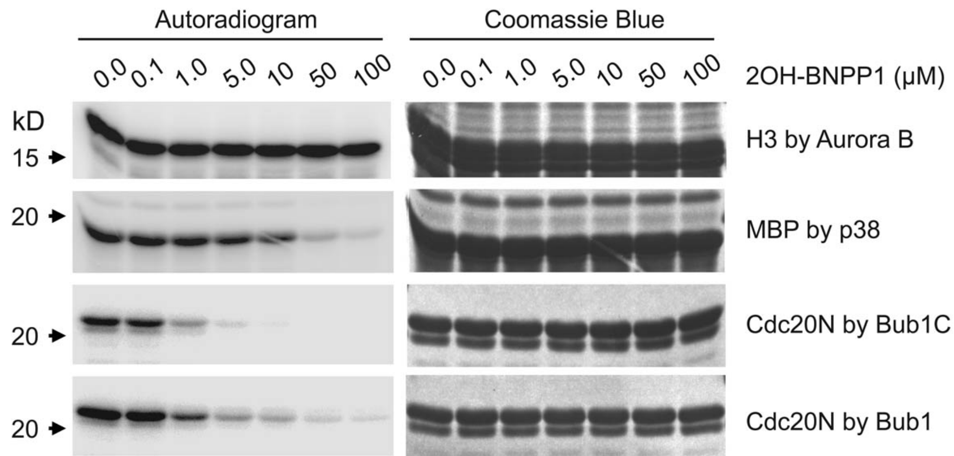

Figure S3. Inhibition of Human Bub1 by the Adenine Analogue, 2OH-BNPP1
Increasing concentrations of 2OH-BNPP1 were added to in vitro kinase reactions of Aurora B (with histone H3 as the substrate), p38 (with myelin basic protein as the substrate), Bub1C and Bub1 (with the N-terminal fragment of Cdc20 as the substrate). The reaction mixtures were separated by SDS-PAGE and analyzed by Coomassie staining followed by autoradiography.

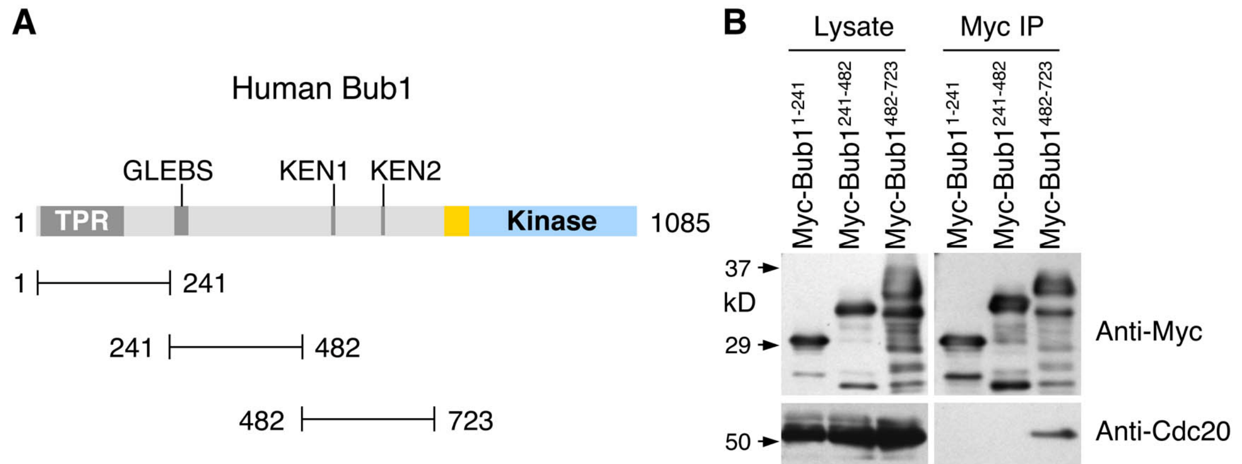

Figure S4. A Bub1 Fragment Containing the KEN Boxes Binds to Cdc20
(A) Schematic drawing of the domain architecture of human Bub1 with the positions of the Bub1 fragments indicated.
(B) HeLa cells were transfected with the indicated plasmids and treated with nocodazole. The cell lysates were IPed with anti-Myc. Both the lysates and Myc IP were blotted with anti-Myc (top panels) and anti-Cdc20 (bottom panels).

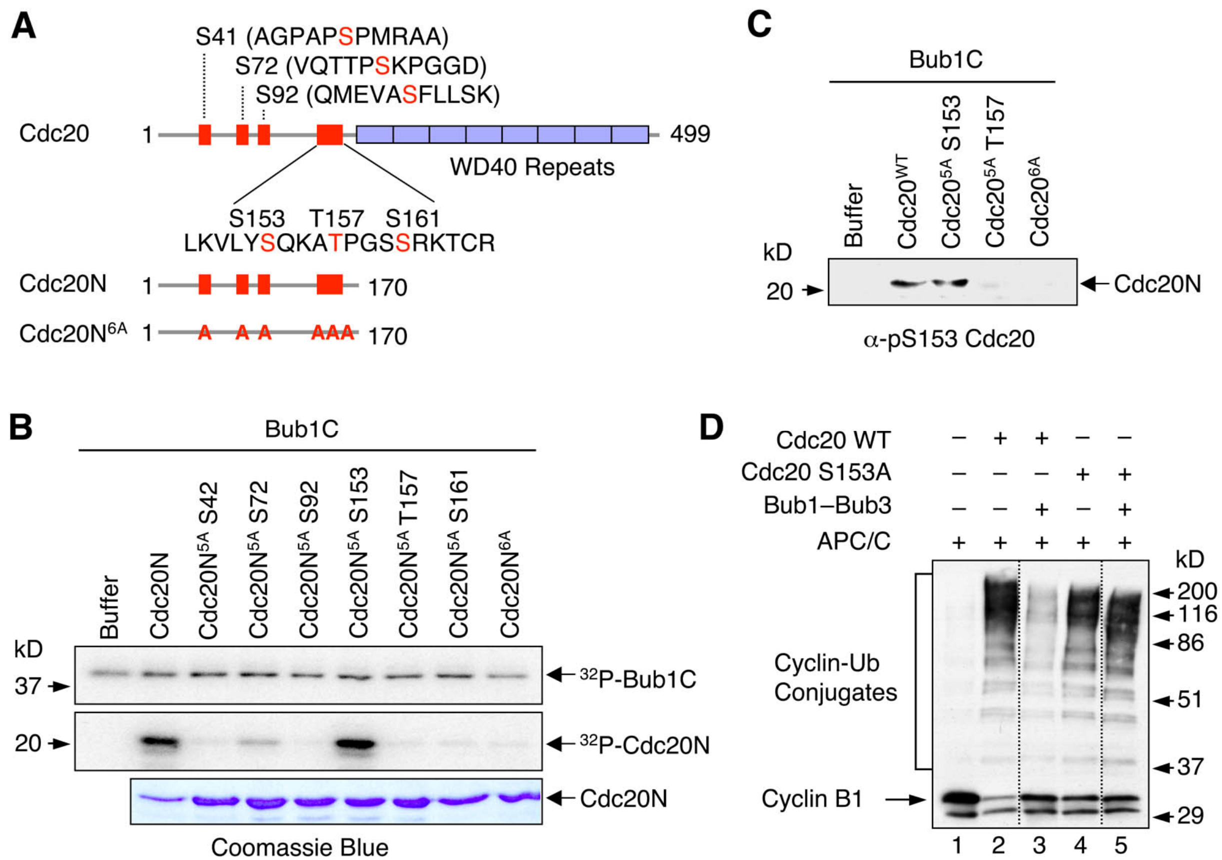

Figure S5. S153 Is a Major Bub1 Phosphorylation Site in Cdc20

(A) Schematic drawing of the domain architecture of human Cdc20 with its phosphorylation sites indicated.

(B) In vitro kinase assays of Bub1C using various Cdc20N mutants as the substrates. ^{32}P-labeled Bub1C, ^{32}P-labeled Cdc20N, and Coomassie-blue stained Cdc20N are shown in the top, middle, and bottom panels, respectively.

(C) The indicated Cdc20N proteins were incubated with Bub1C in the presence of ATP and blotted with anti-phospho-S153 Cdc20.

(D) S153 phosphorylation of Cdc20 is critical for inhibition of APC/C^{Cdc20} by Bub1. Purified recombinant Cdc20 wild-type (WT) and S153A were incubated with purified recombinant Bub1–Bub3 complex in the presence of ATP and added to APC/C isolated from *Xenopus* egg extracts with anti-Cdc27/APC3 beads. The ubiquitin ligase activity of APC/C^{Cdc20} was then assayed using an Myc-tagged N-terminal fragment of human cyclin B1 as the substrate and shown by anti-Myc antibody blotting. The positions of the unmodified cyclin B1 and cyclin B1–ubiquitin (Ub) conjugates are labeled.

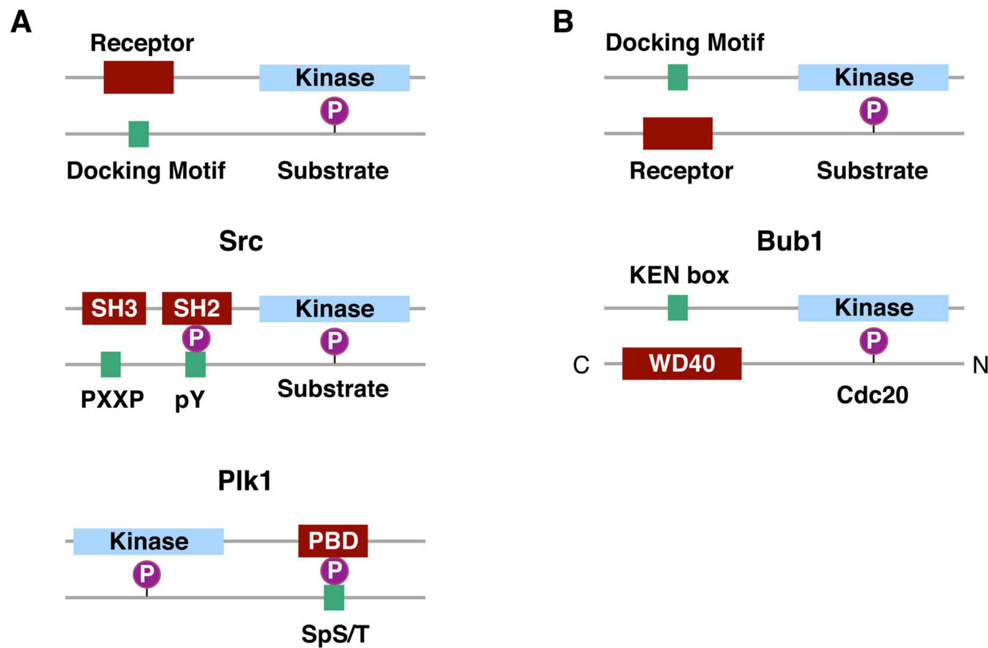

Figure S6. Two Different Modes of Docking Interactions between Kinases and Substrates.
(A) Kinases contain receptors for docking motifs in substrates. SH2, Src homology 2; SH3, Src homology 3; PXXP, proline-rich motif; pY, phospho-tyrosine; PBD, polo-box domain; SpS/T, serine-phospho-serine/threonine.
(B) A novel mode of docking interactions between kinases and substrates exemplified by Bub1 and Cdc20. In this case, substrates contain receptors for docking motifs in kinases.